Research Square

Preprints are preliminary reports that have not undergone peer review.
They should not be considered conclusive, used to inform clinical practice,
or referenced by the media as validated information.

Mild COVID-19 presentations in unexposed individuals favour development of long-lived immune responses to SARS-CoV-2

Danielle I. Stanisic
Griffith University
Lisa J. Ioannidis
The University of Melbourne
Stephanie I. Studniberg
Monash University
Mariam Bafit
Monash University
Victoria Ozberk
Griffith University
Ailin Lepletier
Griffith University
Mei-Fong Ho
Griffith University
Mark Burgess
Griffith University
John Gerrard
Gold Coast Hospital
James Williams
Gold Coast Hospital
Laetitia Hattingh
Gold Coast Hospital
Manisha Pandey
Gold Coast Hospital
Michael F. Good
Griffith University
Diana S. Hansen
diana.hansen@monash.edu

Monash University

Research Article

Keywords: COVID-19, immunity, uncomplicated disease

Posted Date: November 11th, 2026

DOI: https://doi.org/10.21203/rs.3.rs-11495904/v1

License: This work is licensed under a Creative Commons Attribution 4.0 International License.
Read Full License

Additional Declarations: No competing interests reported.

Abstract

Background

Coronavirus disease 2019 (COVID-19), originally reported in Wuhan, China in December 2019 rapidly spread throughout the world resulting in a global pandemic from March 2020. Caused by infection with severe acute respiratory syndrome coronavirus 2 (SARS-CoV-2), the clinical spectrum ranges from asymptomatic to severe and fatal disease. Most patients experience uncomplicated disease, with a wide range of clinical presentations including, headache, fever, cough, dyspnea, sore throat, fatigue, asnomia, myalgia, abdominal pain, diarrhea and nausea. It is well documented that immune responses to SARS-CoV-2 contribute to both immune protection and pathogenesis. Although much useful research has focussed on immune responses predisposing to severe COVID-19, much less is known on whether diverse uncomplicated disease presentations influence the quality and/or magnitude of the immune response to the virus.

Methods

To address this knowledge gap, we pursued a systems immunology approach integrating high dimensional mass cytometry and cytokine responses after SARS-CoV-2 re-stimulation of peripheral blood mononuclear cells (PBMC) from a retrospective study conducted in Australia in 2020.

Results

Cell populations identified by mass cytometry significantly expanding in response to spike-protein *in vitro* stimulation segregated the cohort in patients having ≥ 4 or ≤ 3 symptoms. Cell populations featured by patients with no more than 3 symptoms included $CCR7^{+}$ T_{H2} cells, T_{H2}-polarised T_{FH} cells, along with IgM^{+} classical memory B cells and $CXCR3^{low}$, $CD10^{low}$ classical monocytes. Notably, these responses persisted for 6 months post-exposure, in the absence of new infections.

Conclusions

Together, our results suggest that in previously COVID-19 naïve individuals, mild COVID-19 presentations might support the development of long-lasting immunity to SARS-CoV-2, able to contribute to protection during re-infection.

Background

Coronavirus disease 2019 (COVID-19) was originally reported in Wuhan, China in December 2019 with subsequent, rapid spread resulting in the declaration of a global pandemic on 12 March 2020. Caused by

infection with severe acute respiratory syndrome coronavirus 2 (SARS-CoV-2), the clinical spectrum ranges from asymptomatic to severe and fatal disease; however, most patients experience uncomplicated disease [1]. While COVID-19 predominantly presents as a respiratory illness, more systemic clinical presentations are also observed. Symptoms include headache, fever, cough, dyspnea, sore throat, fatigue, anosmia, myalgia, abdominal pain, diarrhea and nausea. Long COVID (LC) describes the phenomenon of symptom persistence for > 12 weeks after the initial infection [2].

Immune responses induced to SARS-CoV-2 during acute infection contribute to both immune protection and pathogenesis [3, 4]. Following uncomplicated mild disease, IgG, IgA and neutralizing antibody responses can be detected [5, 6] as well as $CD4^+$ and $CD8^+$ T cells specific for several essential SARS-CoV-2 structural proteins including the spike glycoprotein [6], which is essential for attachment to the entry receptor angiotensin-converting enzyme 2 (ACE2) on the surface of host cells [7]. These immune responses may play a role in protection from re-infection. Inflammation and dysregulation of innate and adaptive immune responses during the acute phase of infection, however, can contribute to tissue destruction and pathogenesis and the development of severe disease [8]. Interestingly, cross-reactive SARS-CoV-2 $CD4^+$ T cell memory responses have been detected in non-exposed, healthy individuals, although it is unclear whether this immunity can modify clinical outcomes during subsequent COVID-19 infections.

Numerous studies have investigated the immune response during and after SARS-CoV-2 infection to better understand the immune mechanisms underlying the variable clinical presentations between patients (e.g. [8–10] and the long-term impact of the infection on the immune system [11]). This information may assist in the rational design of novel preventives and therapeutic interventions. Although much useful research has focussed on immune responses during severe COVID-19, much less is known on whether diverse uncomplicated disease presentations influence the quality and/or magnitude of the immune response to SARS-CoV-2. In this study, we employed high dimensional mass cytometry to characterise spike protein-specific cellular immune responses during the convalescence phase of mild COVID-19, the longevity of these responses and their associations with diverse clinical presentations during acute infection. Our main results revealed that patients experiencing no more than three disease symptoms preferentially featured populations of classical monocytes, IgM^+ memory B cells (MBCs) and a T_{H2} polarised response against the virus compared that persisted for 6 months after exposure, suggesting that mild infection might predispose the development of more long-lasting immunity able to contribute to protection during re-infection.

Methods

Study design. Twenty-nine convalescent COVID-19 subjects were recruited for this study at Gold Coast University Hospital between April and August 2020 [12]. Disease severity at the time of initial presentation was categorised according to “Clinical management of COVID-19: interim guidance, 27 May 2020” [13]. Twenty-two patients were categorised as having uncomplicated COVID-19 and were selected for this study. Venous blood was collected from consenting participants at enrolment (3–6 weeks after

recovery) into BD Vacutainer CPT tubes (BD Biosciences, Franklin Lakes, NJ, USA). Within four hours of blood collection, peripheral blood mononuclear cells (PBMCs) were isolated using BD Vacutainer® CPT™ Mononuclear Cell Preparation Tubes according to manufacturer's instructions and cryopreserved until analysis. An additional venous sample was also collected from eight participants at approximately 6 months after recovery. Healthy donor PBMCs (n = 9), collected pre-COVID-19, were also isolated from buffy packs obtained from the Australian Red Cross LifeBlood. All blood samples were collected prior to the availability of SARS-CoV-2 vaccines. This study was approved by the Human Research Ethics Committees of the Gold Coast University Hospital (HREC/20/QGC/63284), Griffith University (HREC/GU/2018/936), the Walter and Eliza Hall Institute of Medical Research (HRECG20/21) and Monash University (HREC36410). Written informed consent was obtained from all study participants prior to their inclusion in the study. All the experiments conformed to the principles set out in the WMA Declaration of Helsinki and the Department of Health and Human Services Belmont Report.

In vitro restimulation of PBMCs. Cryopreserved PBMCs were thawed in complete medium (RPMI 1640 with 25mM HEPES, 10% heat-inactivated foetal bovine serum [HI-FBS; Sigma], 100 U/mL penicillin, 100 µg/mL streptomycin and 2mM L-glutamine), counted and then seeded into U-bottom 96-well plates ($5x10^5$ cells/well). PBMCs were then stimulated with 5µg/mL of recombinant SARS-CoV-2 spike protein or media alone for 20 hours at 37°C with 5% CO_2.

Cytometry by time of flight (CyTOF). After stimulation, cells were incubated for 10 min on ice with PBS containing 10mM glucose and 3mM ethylenediaminetetraacetic acid (EDTA) to detach adherent cells. Unstimulated and spike-stimulated PBMCs ($2x10^6$) were then stained with 5mM Cell-ID Cisplatin (Fluidigm) in PBS for 5 minutes at room temperature. Cells were then blocked with Human TruStain FcX (Biolegend) and stained with a cocktail of surface marker antibodies (Table S1) in CyTOF staining buffer (PBS with 0.5% bovine serum albumin [BSA; Sigma] and 0.02% sodium azide [Sigma]) for 30 minutes at room temperature. After staining, cells were washed twice with CyTOF staining buffer and stored in Maxpar fix and perm buffer (Fluidigm) with 125nM Cell-ID iridium intercalator (Fluidigm) for a minimum of 18 hours at 4°C. Prior to data acquisition, cells were washed twice by centrifugation in ultrapure water and then resuspended in a 1/10 dilution of 4-Element EQ normalization beads (Fluidigm) in ultrapure water. Cells were analysed on a Helios model mass cytometer (Fluidigm) at ~ 300 events/second. Data were normalized using the signal from 4-Element EQ Beads (Fluidigm) as previously described [14]. Manual gating was then performed using FlowJo version 10 (BD Biosciences) to exclude doublets and dead cells, before individual cell populations were selected and exported for further analysis in Cytobank [15]. Individual cell populations were then visualized using viSNE [16], while FlowSOM [17] was used to identify cell sub-populations. The following parameters (Table S2) were included in the viSNE (vi-Stochastic Neighbor Embedding) analysis for MBCs: Immunoglobulin (Ig)D, IgM, IgA, CXC chemokine receptor (CXCR)5, CXCR3, CC chemokine receptor (CCR)6, CCR7, CD45RA, CD21 and CD27. For memory $CD8^+$ T cells as well as T_{H1}-, T_{H2}- and T_{H17}-like memory $CD4^+$ T cells the following parameters were included: CXCR5, CCR7, PD-1, ICOS, CD25, CD27 and CD127. For memory T_{FH} cells the following parameters were included: CXCR3, CCR6, ICOS, PD-1, CD27, CD25 and CD127. For monocytes subsets,

the following parameters were included: CD16, CXCR3, CD4, CD8, CD10, CD27, CD45RA, CD56 and CD127. Self-organizing maps (SOMs) were then generated for each cell population using equal event sampling and hierarchical consensus clustering on the t-Distributed Stochastic Neighbor Embedding (tSNE) axes. CITRUS was used to identify differentially abundant cell populations using the same parameters as the viSNE analysis. For each pairwise CITRUS analysis [18], equal event sampling was used and the Significance Analysis of Microarrays (SAM) model with a 5% False Discovery Rate (FDR) was applied.

Cytometric Bead Arrays. After stimulation, cell culture supernatants were collected, clarified by centrifugation and then stored at -80°C until assayed. Interferon- γ (IFN-γ), tumour necrosis factor (TNF), interleukin (IL)-10, IL-6, IL-4, IL-2 and IL-17A levels were then measured in culture supernatants using a Human Th1/Th2/Th17 CBA Kit (BD Biosciences) according to manufacturer's instructions and an LSR Fortessa FACS Diva flow cytometer. Data were analysed using FCAP Array software version 3.0.1 (BD Biosciences).

Flow Cytometry. Cryopreserved PBMCs (1-2x10^6) were thawed in complete medium, washed twice with PBS and stained with a 1/1000 dilution of Fixable viability dye eFluor 506 (eBioscience) in PBS for 25 minutes on ice. Cells were then washed twice with FACS buffer (PBS with 1% HI-FBS and 2mM ethylenediaminetetraacetic acid [EDTA; Sigma]), blocked with Human TruStain FcX (Biolegend) and stained with a cocktail of surface marker antibodies (Table S3) and PE-conjugated SARS-CoV-2 spike protein for 45 minutes on ice as previously described [19]. Cells were then washed twice, fixed with 2% paraformaldehyde (Sigma) and analysed on a BD Fortessa X-20. Data analysis was performed using FlowJo version 10 (BD).

Statistical analysis. Characteristics and endpoints of clinical groups were compared using unpaired t-test or ANOVA with Tukey's multiple comparisons for continuous data that were normally distributed, while the Mann-Whitney test with correction for multiple comparisons was used for data that did not follow normal distribution. Correlations were calculated using the Spearman's rank correlation coefficient and visualised under a force directed organic layout using Cytoscape v3.10.0. Unsupervised clustering and principal component analysis of cellular responses was performed in ClustVis using the average clustering method (https://biit.cs.ut.ee/clustvis/). Statistical analyses were performed in GraphPad prism v9.0.

Results

Cohort characteristics

The study recruited individuals with a confirmed COVID-19 positive diagnosis between April-August 2020. Consenting participants donated a venous blood sample at convalescence (3–6 weeks after recovery). Twenty-two participants with uncomplicated disease were selected for this study. Their demographic and clinical characteristics are summarised in Table 1. The cohort was comprised of equal

numbers of males and females with a median age of 59 years (range 21–81 years). Cough (86.36%) and fever (63.63%) were the most prevalent symptoms at presentation. Other prevalent symptoms included rhinorrhea (50%), sore throat (40.9%), headache (40.9%), fatigue (36.36%), malaise (31.82%), anosmia (27.27%) and ageusia (22.72%). Antibody responses to SARS-CoV-2 have previously been previously reported in this cohort [12].

Table 1
Demographic characteristics and symptoms of participants with COVID-19

Demographics	
Total, *n*	22
Age, years, median (range)	59 (21–81)
Male, *n*	11
Female, *n*	11
Date of symptom onset, range	14 March 2020-10 April 2020
Symptoms (n; %)	
Fever	14; 63.63
Shortness of breath*	2; 9.52
Cough	19; 86.36
Sore throat	9; 40.90
Rhinorrhea	11; 50
Nasal congestion	4; 18.18
Ageusia	5; 22.72
Anosmia	6; 27.27
Headache	9; 40.90
Diarrhea	4, 18.18
Nausea/vomiting	1; 4.54
Fatigue	8; 36.36
Malaise	7; 31.81
* data missing for one participant	

High-dimensional mass cytometry identifies lymphocyte sub-populations expanding in response to SARS-CoV-2 in convalescent COVID-19 cases

To identify lymphocyte sub-populations associated with different COVID-19 presentations, PBMCs of study participants collected at convalescence (~ 3 weeks after confirmed diagnosis) were stimulated *in vitro* with SARS-CoV-2 recombinant spike protein as described in Methods. PBMCs were then stained with a panel of metal-labelled antibodies against a range of B cell, $CD4^+$ T cell, $CD8^+$ T cell, Natural Killer (NK) cell and monocyte markers (Table S1) and analysed by cytometry by time of flight (CyTOF). Cells from unexposed individuals (collected before December 2019) were used as controls.

Within the circulating memory $CD4^+$ T cell compartment, surface expression of the chemokine receptors CCR6 and CXCR3 allows the identification of T helper $(T_H)_1$-like ($CCR6^-CXCR3^+$), T_{H2}-like ($CCR6^-CXCR3^-$) and T_{H17}-like ($CCR6^+CXCR3^-$) cells, while circulating memory T follicular helper (T_{FH}) cells can be identified by expression of CXCR5 (Additional file 1: Fig. S1). To explore the composition of these memory $CD4^+$ T cell populations, tSNE analysis and FlowSOM clustering were performed, and marker expression was assessed in each cell population in unexposed or COVID-19 convalescent individuals after *in vitro* stimulation with recombinant spike protein (Fig. 1). This approach allowed for the identification of five-six distinct sub-populations of T_{H1} memory $CD4^+$T cells (Fig. 1A), T_{H2} memory $CD4^+$ T cells (Fig. 1B), T_{H17} memory $CD4^+$ T cells (Fig. 1C) and memory T_{FH} cells (Fig. 1D) expressing variable levels of chemokine receptors and surface markers including CCR7, ICOS, PD-1, CD25, CD27 and CD127. A similar approach was used to explore the composition of the memory $CD8^+$ T cell pool, with six distinct sub-populations identified (Fig. 1E).

Within the innate cell compartment, FlowSOM clustering of gated $CD14^+$ monocytes (Additional file 1: Fig. S1) revealed two classical ($CD14^+CD16^-$), one intermediate ($CD14^+CD16^{low}$) and three non-classical ($CD14^+CD16^{high}$) monocyte sub-populations (Fig. 1. F) in the blood of convalescent COVID-19 patients.

Memory B cells (MBCs) did not change in frequency after SARS-CoV-2 spike stimulation, thus the *ex vivo* frequencies of unexposed controls and COVID-19 convalescent unstimulated cells are shown in Fig. 1G. tSNE analysis and FlowSOM clustering of gated $CD19^+CD20^+CD10^-$ cells allowed the identification of 8 subsets of MBCs, including 5 clusters of classical MBCs ($CD27^+CD21^+$), one population of activated MBCs ($CD27^+CD21^-$) and two populations of atypical MBCs ($CD27^-CD21^-$).

The frequency of each cell sub-population identified by FlowSOM clustering was determined for each clinical group. Three weeks after infection with SARS-CoV-2, multi-dimensional scaling and unsupervised clustering of all FlowSOM clusters prior to SARS-CoV-2 spike stimulation partially segregated unexposed from COVID-19 convalescent individuals (Additional file 2: Fig. S2). As illustrated in Fig. 1A-G, these differences became more apparent after recombinant SARS-Co-V-2 spike protein *in vitro* stimulation, with unsupervised hierarchical clustering (Fig. 1H) and multi-dimensional scaling (Fig. 1I) of all sub-

populations displaying a very good level of segregation between unexposed individuals and COVID-19 convalescent cases. As depicted in the heatmap (Fig. 1H), three main groups of cell populations were identified by this analysis, with cell populations more abundant in COVID-19 cases in clusters 1 and 2, and cell populations preferentially expressed among healthy controls in cluster 3 (Fig. 1I).

To further explore these responses, unsupervised identification of cell populations significantly expanding (FDR < 5%) in response to SARS-CoV-2 recombinant spike protein was performed using the CITRUS algorithm [27]. Whereas no populations were detected by this approach within the unexposed control group, this analysis identified a population of $CXCR5^+$ T_{FH} cells expressing inducible T cell costimulatory (ICOS), programmed cell death protein 1 (PD-1) and CD27, as well as a $CCR7^+$, $CD27^+$, subset, consistent with a central memory phenotype, expanding within the $CD4^+$ T_{H1}-polarised T cell pool (Fig. 2A). Interestingly, highly related populations of $ICOS^+PD\text{-}1^+CXCR5^+$ T_{FH} cells and $CCR7^+$, $CD27^+$ central memory cells were also significantly expanded in the T_{H2} and T_{H17} polarised $CD4^+$ T cell pools (Fig. 2B, C). When gated $CXCR5^+$ $CD4^+$ memory T_{FH} cells were analysed, CITRUS revealed a different population in this lineage, expressing CCR7 and CD27 and low PD-1, consistent with a T_{H2} phenotype ($CXCR3^-CCR6^-$) significantly expanded in response to spike (Fig. 2D).

As monocytes do not possess strong proliferating capacity, this compartment was initially analysed prior to spike stimulation. CITRUS analysis revealed a population of $CXCR3^+CD10^+CD16^-$ monocytes, differentially abundant between COVID-19 convalescent and unexposed individuals (Additional file 3: Fig. S3). This cell population did not change in frequency after *in vitro* culture with SARS-CoV-2 spike protein (Fig. 2E). In contrast, spike *in vitro* re-stimulation resulted in significant fluctuations in cell frequencies within other monocyte populations, with two populations of $CD16^+$ non-classical monocytes reduced and a cluster of $CXCR3^{low}CD10^{low}$ classical monocytes more abundant after spike stimulation compared to unstimulated controls (Fig. 2E).

A population of IgM^+ IgD^{low} MBCs, expressing high levels of CXCR5 and CCR6 was found to be differentially abundant between COVID-19 convalescent and unexposed clinical groups in unstimulated cultures (Fig. 2F). Consistent with these findings, flow cytometry analysis using a SARS-CoV-2 spike-specific B cell probe identified IgM^+ MBCs as the main population of virus-specific B cells present within PBMCs in COVID-19 convalescent samples (Additional file 4: Fig. S4), implying that cells revealed by our CITRUS analysis are specific for SARS-CoV-2. Thus, at convalescence, COVID-19 uncomplicated cases feature a range of $CD4^+$ T cells of different polarisation, along with IgM^+ MBCs and a defined subset of classical monocytes, able to recognise and respond to SARS-CoV-2 cognate antigen stimulation.

Defined cellular responses to infection associate with different COVID-19 clinical presentations

In the next series of experiments, cytokine responses to spike stimulation were assessed in cell culture supernatants following *in vitro* culture of PBMCs from the study participants. In general, IL-2 responses were low in both controls and COVID-19 cases but IFN-γ responses were significantly higher in this group compared to unexposed individuals (Fig. 3A). Interestingly, similar levels of IL-10, IL-6 and TNF could be detected among COVID-19 cases and unexposed controls, presumably reflecting innate cell populations in the latter group secreting cytokine upon a primary encounter with viral antigen (Fig. 3A).

To reveal associations between cytokine responses and cell populations significantly expanding in response to virus-specific restimulation in COVID-19 convalescent individuals, a model was constructed using Spearman correlations between differentially abundant populations identified by CITRUS and cytokine responses (Fig. 3B). Under force directed organic layout based on correlation strength, a well organised cluster formed around IL-6, IL-10 and TNF responses that were highly correlated with each other (Fig. 3B). Interestingly, whereas populations of T_{H1}, T_{H2} and T_{H17}-polarised $CXCR5^{+}ICOS^{+}$ cells were highly associated with each other, a separate cluster of cell populations including T_{H1}, T_{H2} and T_{H17}-polarised $CCR7^{+}$ $CD4^{+}$ memory cells, IgM^{+} MBCs, T_{H2}-like T_{FH} cells and $CXCR3^{low}$ $CD10^{low}$ classical monocytes, was negatively associated with these cell types (Fig. 3B).

Since uncomplicated COVID-19 that does not require hospitalisation presents as a wide range of diverse clinical symptoms, we then sought to determine whether our systems approach could reveal specific responses to infection associated with different disease presentations. Clinical information from the participants revealed mainly 12 defined COVID-19 symptoms present in the cohort study as shown in Table 1. Spearman correlations between the incidence of these symptoms visualised under a force directed organic layout allowed the identification of two clusters of symptoms, where respiratory tract presentations, including sore throat, cough and loss of taste were correlated with each other and symptoms consistent with a more systemic COVID-19 presentation including, fatigue, malaise, fever, headache and nausea, were highly associated with each other (Fig. 4A). Furthermore, contingency analysis of symptoms across study participants allowed division of the cohort in 2 groups having ≤ 3 or ≥ 4 symptoms. Whereas the first group included cases with only respiratory tract associated presentations, the second group consisted of cases that developed a more severe disease, experiencing both respiratory tract and systemic presentations (Fig. 4B). Interestingly, unsupervised hierarchical clustering of cell populations significantly more abundant after spike-specific stimulation identified in Fig. 2 at convalescence provided a good level of segregation of cases experiencing ≤ 3 or ≥ 4 COVID-19 symptoms. Two groups of responses were identified by this analysis (Fig. 4C), with TNF, IL-10 and $CXCR5^{+}ICOS^{high}$ T_{H1}, T_{H2} and T_{H17} cells (highly correlated to each other in Fig. 3B) more abundant in cases with ≥ 4 symptoms, and $CCR7^{+}ICOS^{+}$ T_{H1}, T_{H2}, T_{H17} and T_{FH} cells, along with IgM^{+} classical MBCs and $CXCR3^{low}$, $CD10^{low}$ classical monocytes (highly correlated to each other in Fig. 3B) more abundant in COVID-19 milder presentations (Fig. 4C). Furthermore, while a population of T_{H1}-polarised $CXCR5^{+}ICOS^{+}$ cells was significantly more elevated in individuals with ≥ 4 symptoms after correcting for multiple comparisons, the percentage of $CXCR3^{low}$ $CD10^{low}$ classical monocytes, more abundant after spike

stimulation at convalescence, was significantly higher in mild cases with ≤ 3, compared to those with more complex presentations with ≥ 4 symptoms (Fig. 4D). Thus, this approach identified responses preferentially activated in mild COVID-19 presentations, suggesting an association between defined populations of classical monocytes and protection from systemic COVID-19 presentations in naïve patients.

Mild COVID-19 presentations in naïve individuals favour long-lived immune responses to SARS-CoV-2

To investigate the longevity of immune responses to SARS-CoV-2 in cases with different clinical presentations, PBMCs from study participants collected 6 months after initial infection with the virus (n = 8) were stimulated with recombinant spike protein, stained with a panel of metal labelled antibodies and analysed by CyTOF as described above. Unsupervised identification of cell populations significantly expanding (FDR < 5%) in response to SARS-CoV-2 recombinant spike protein identified populations of $CCR7^+$, $CD27^+$, $CD4^+$ T_{H2}-polarised T cells (Fig. 5A) but not the T_{H1} or T_{H17} polarised cells, that expanded in response to *in vitro* re-stimulation 3 weeks post-infection. CITRUS analysis also revealed the expansion of a population of $CD4^+$ T_{H2}-polarised memory T_{FH} cells, expressing high levels of CCR7 and CD27 (Fig. 5B).

By 6 months post-infection no differences were found in the cellular composition of the monocyte compartment between COVID-19 cases and unexposed controls. Similar to the results at convalescence though, spike protein *in vitro* re-stimulation at 6 months post-infection resulted in significant fluctuations in the monocyte compartment (Fig. 5C), with a cluster of $CD4^+CD16^+$ non-classical monocytes reduced and a cluster of $CXCR3^{low}CD10^{low}$ classical monocytes more abundant compared to unstimulated controls. Lastly, IgM^+ IgD^{low} MBCs, expressing high levels of CXCR5 and CCR6 were differentially abundant between COVID-19 cases 6 months after infection and unexposed clinical groups (Fig. 5D). Interestingly, all cellular responses to the virus found 6 months after exposure were found to be correlated with each other during convalescence (Fig. 3B) and more abundant in cases with ≤ 3 compared to those with ≥ 4 COVID-19 symptoms (Fig. 4C, D). As observed 3 weeks post-infection, IFN-γ responses to spike stimulation in cell culture supernatants were significantly higher in COVID-19 cases compared to unexposed individuals after 6 months, with similar levels of IL-10, IL-6 and TNF found among exposed and unexposed controls (Fig. 5E).

To provide a more thorough kinetic analysis of cellular responses after exposure to the virus over time, the frequencies of FlowSOM clusters defined in Fig. 1 aligned with the phenotypes of cell populations revealed by unsupervised CITRUS analysis in Fig. 2 were calculated. Whereas no expansion of $CCR7^+$ $CD27^+$ T_{H2} cells (Fig. 5F), $CCR7^+CD27^+$ T_{H2}-polarised T_{FH} cells (Fig. 5G) nor $CXCR3^{low}$ $CD10^{low}$ classical monocytes (Fig. 5H) was observed in unexposed individuals after spike stimulation, cells from COVID-19 cases showed a response of similar magnitude 3 weeks and 6 months post-infection (Fig. 5F-H).

Furthermore, frequencies of IgM^+ MBCs upregulated immediately after exposure, persisted for 6 months in the absence of new infections (Fig. 5I). Noteworthy, multi-dimensional scaling (Fig. 5J) and unsupervised hierarchical clustering (Fig. 5K) of responses persisting 6 months after exposure clearly segregated COVID-19 cases with ≤ 3 from ≥ 4 disease symptoms, even in a small cohort (n = 8) of patients that participated in the follow up period, with all cellular responses appearing more abundant in individuals with ≤ 3 COVID-19 symptoms. Thus, together these results are consistent with the notion that in SARS-CoV-2 naïve individuals, mild presentations of COVID-19 (≤ 3 symptoms) are conducive to the development of more long-lived cellular responses to infection.

Discussion

Despite extensive investigation of immune responses in severe COVID-19, the extent to which variability within uncomplicated COVID-19 presentations is associated with the magnitude, functional quality, and durability of SARS-CoV-2–specific immune responses remains an important and incompletely defined gap with direct relevance to vaccine development. Here, we used high dimensional mass cytometry, flow cytometry and cytometric bead arrays to identify immune cell populations that expanded in response to SARS-CoV-2 spike protein in individuals recovering from uncomplicated COVID-19, and to determine how these responses relate to clinical disease and immune durability.

IgM^+ MBCs are an antigen-experienced yet unswitched MBC subset that retains IgM expression. They are proposed to support rapid recall responses with broad antigen recognition, distinct from conventional class-switched memory B cells. The pentameric structure of secreted IgM favours strong binding to pathogens, making it highly effective at neutralizing pathogens and activating the complement system. At convalescence, IgM^+ MBCs were the dominant SARS-CoV-2-specific B cell population and these cells persisted for at least 6 months in the absence of re-exposure. They were more relatively abundant in individuals with ≤ 3 symptoms (i.e. those with milder disease). A robust IgM^+ MBC response has previously been associated with milder, more rapidly resolving forms of COVID-19, with reductions in this subset correlated with more severe disease (reviewed in [20]). In non-hospitalised and mildly symptomatic individuals, preservation of unswitched IgM^+ MBC populations during convalescence was demonstrated, with higher frequencies associated with shorter symptom duration and favourable clinical resolution [21]. IgM^+ MBCs may therefore represent an underappreciated component of SARS-CoV-2 immunity, particularly following uncomplicated infection. It has also been shown that IgM mAbs generated from antigen-experienced IgM^+ MBCs derived from convalescent donors can have potent SARS-CoV-2 neutralising activity [22]. Together, these observations suggest that IgM^+ MBCs may serve as a marker, and potentially a mediator, of effective humoral immune memory after uncomplicated SARS-CoV-2 infection, although their precise role in long-term protection and recall responses requires further investigation.

At convalescence, central memory $CD4^+$ T cells across the T_{H1}, T_{H2} and T_{H17} lineages were observed, including populations of activated T_{FH} cells. At 6 months, only the $CCR7^+$ $CD27^+$ T_{H2}-polarised $CD4^+$ T

cells and T_{H2}-like T_{FH} cells persisted. Central memory T cells have high proliferative capacity, are long-lived, rapidly expand and differentiate into effector cells upon antigen re-exposure and therefore have capability to contribute to protection following re-infection [23]. $CXCR5^+$ T_{FH} cells were one of the most durable, consistently expanding spike-responsive populations that we observed in individuals with mild clinical presentations. A strong T_{FH} response is generally associated with better antibody responses, and their persistence suggests ongoing/recallable help for antibody responses [10, 24].

The observation that only T_{H2}-polarised $CD4^+$ T-cell responses were detectable six months after infection suggests selective survival of long-lived memory populations rather than persistence of active anti-viral responses. T_{H2} memory cells are capable of long-term persistence following antigen clearance and retain potent recall capacity through stable lineage-specific programming. Because T_{H1} responses are typically more closely associated with inflammatory cytokine environments generated during intracellular infection, T_{H2}-skewed memory populations may preferentially persist after viral clearance, particularly when infection is mild or rapidly resolved [25–27]. It is also possible that these results may reflect the tissue redistribution of different $CD4^+$ T cell populations following viral infection. Anti-viral T_{H1}-polarised $CD4^+$ T cells preferentially migrate to non-lymphoid tissues and establish long-lived tissue-resident memory populations, particularly within sites of prior infection such as the respiratory tract, resulting in their relative under-representation in the circulation after viral clearance [28, 29]. In contrast, T_{H2}-polarised cells may be relatively enriched within the circulating memory pool. Consequently, analyses of peripheral blood months after infection may underrepresent T_{H1} immunity and suggest an apparent T_{H2} bias that reflects differential tissue redistribution rather than immune skewing.

Notably, *in vitro* restimulation with SARS-CoV-2 not only resulted in expansion of virus-specific T cells but also had an impact in the blood innate cell compartment with apparent reductions in the frequency of non-classical monocytes and an increase in the proportion of classical monocytes expressing low levels of CXCR3 and CD10. Interestingly, these responses were detected both 3 weeks and even 6 months after infection with SARS-CoV-2 but not in the blood compartment of naïve individuals collected before December 2019 and appeared to be significantly higher in patients with mild disease presentation. Although a bystander activation by cytokines produced by cell types other than monocytes produced during *in vitro* stimulation cannot be excluded, our results suggest that a cognate interaction between SARS-Co-V-2 spike protein and monocytes and an altered ability of these cells to respond to this stimulus after initial exposure to the virus might be responsible for this process. Consistent with these findings, SARS-Co-V-2 spike has been shown to activate blood monocytes [30, 31], and trained immunity of this innate cell population has been documented to occur during COVID-19 [32, 33]. The clinical implications of this monocyte trained immunity during COVID-19 are not fully understood, with evidence suggesting that upon re-exposure, these cells could be implicated in detrimental [34, 35] or protective [33] responses. In this study, the increased frequency of CXCR3-expressing classical monocytes was evident in mild COVID-19 presentations (less than 3 symptoms) after a primary exposure to SARS-Co-V2, suggesting a potential protective effect of these cells in the control of viral replication and/or alleviation

of disease symptoms. Whether the apparent expansion of these cells upon *in vitro* SARS-Co-V spike re-stimulation reflected an enrichment due to decreased proportions of other monocytes subsets, the differentiation from other CXCR3-expressing monocytes in the blood or a proliferative response cannot be fully inferred from this study. In support of the latter though, $CXCR3^+$ monocytes known to have strong tissue homing capacity have been previously detected in COVID-19 convalescent individuals [36], and it has been documented that monocytes undergo a short period of expansion prior to their localisation in tissue and differentiation into macrophages [37].

Conclusions

In conclusion, in SARS-CoV-2–naïve individuals, uncomplicated COVID-19 was associated at convalescence with a coordinated immune response involving central memory $CD4^+$ T cells and T_{FH} cells, IgM^+ MBCs, and classical monocytes that responded robustly to spike antigen, persisted for at least six months and were preferentially observed in conjunction with reduced systemic disease. Durable responses were enriched in individuals with mild disease (≤ 3 symptoms). This suggests that mild clinical presentations might favour the development of long-lived, cellular immunity that may offer protection against SARS-CoV-2 re-infection. Although some of the limitations of the study include a small sample size, particularly during the 6 month time-point, and/or an extended follow up beyond this point, our findings have implications for COVID-19 vaccine development by highlighting immune components that may contribute to non-pathogenic and long-lasting immunity to SARS-CoV-2, including the importance of inducing long-lived central memory responses rather than highly activated, short-lived effector phenotypes linked to inflammation.

Abbreviations

SARS-CoV-2
severe acute respiratory syndrome coronavirus 2
COVID-19
coronavirus disease 19
ACE2
angiotensin-converting enzyme 2
PBMCs
peripheral blood mononuclear cells
CyTOF
cytometry by time of flight
LC
long COVID
vi-SNE
vi- Stochastic Neighbour Embedding
t-SNE

t-Distributed Stochastic Neighbour Embedding
SAM
Significance Analysis of Microarray
SOM
Self-organizing map
FDR
false discovery rate
Ig
immunoglobulin
CXCR
CXC chemokine receptor
CCR
CC chemokine receptor
NK cell
natural killer cell
MBCs
memory B cells
T_H cell
T helper cell
T_{FH}
T follicular helper cell
ICOS
inducible T cell costimulatory
PD-1
programmed cell death protein 1
IFN-γ
interferon gamma
TNF
tumour necrosis factor
IL
interleukin

Declarations

Ethics approval and consent to participate:

This study was approved by the Human Research Ethics Committees of the Gold Coast University Hospital (HREC/20/QGC/63284), Griffith University (HREC/GU/2018/936), the Walter and Eliza Hall Institute of Medical Research (HRECG20/21) and Monash University (HREC36410). Written informed consent was obtained from all study participants prior to their inclusion in the study

Consent for publication:

Not applicable.

Competing interests:

The authors declare no competing interests.

Funding:

This work was performed in part at the Materials Characterisation and Fabrication Platform (MCFP) at the University of Melbourne and the Victorian Node of the Australian National Fabrication Facility (ANFF). Supported by the Australian Government National Health and Medical Research Council (NHMRC) Independent Medical Research Institutes Infrastructure Support Scheme and the Victorian State Government Operational Infrastructure Support.

Author Contribution

D.I.S., L.J.I., M.G. and D.S.H. conceived and designed the study. V.O., A.L., M.P., J.G., J.W. and L.H. conducted the field sample collection. D.I.S., L.J.I., M.H. and M.B. performed the experiments. D.I.S., L.J.I., S.I.S., M.B, M.G and D.S.H performed the analysis. D.I.S., L.J.I., and D.S.H. wrote the manuscript. D.I.S. and D.S.H. supervised the study. All authors reviewed the manuscript.

Acknowledgement

We thank donors and patients for participating in this study.

Availability of data and materials:

The datasets used and/or analysed during the current study are available from the corresponding author on reasonable request.

References

1. Wiersinga WJ, Rhodes A, Cheng AC, Peacock SJ, Prescott HC. Pathophysiology, Transmission, Diagnosis, and Treatment of Coronavirus Disease 2019 (COVID-19): A Review. JAMA: J Am Med Association. 2020;324(8):782–93.
2. WHO. Post COVID-19 condition (long COVID). *World Health Organisation* 2022.

3. Purbey PK, Roy K, Gupta S, Paul MK. Mechanistic insight into the protective and pathogenic immune-responses against SARS-CoV-2. Mol Immunol. 2023;156:111–26.
4. Malireddi RKS, Sharma BR, Kanneganti TD. Innate Immunity in Protection and Pathogenesis During Coronavirus Infections and COVID-19. Annu Rev Immunol. 2024;42(1):615–45.
5. Garrido C, Hurst JH, Lorang CG, Aquino JN, Rodriguez J, Pfeiffer TS, Singh T, Semmes EC, Lugo DJ, Rotta AT et al. Asymptomatic or mild symptomatic SARS-CoV-2 infection elicits durable neutralizing antibody responses in children and adolescents. JCI Insight 2021, 6(17).
6. Grifoni A, Weiskopf D, Ramirez SI, Mateus J, Dan JM, Moderbacher CR, Rawlings SA, Sutherland A, Premkumar L, Jadi RS, et al. Targets of T Cell Responses to SARS-CoV-2 Coronavirus in Humans with COVID-19 Disease and Unexposed Individuals. Cell. 2020;181(7):1489–501. e1415.
7. Shang J, Wan Y, Luo C, Ye G, Geng Q, Auerbach A, Li F. Cell entry mechanisms of SARS-CoV-2. Proc Natl Acad Sci U S A. 2020;117(21):11727–34.
8. Nasrollahi H, Talepoor AG, Saleh Z, Eshkevar Vakili M, Heydarinezhad P, Karami N, Noroozi M, Meri S, Kalantar K. Immune responses in mildly versus critically ill COVID-19 patients. Front Immunol. 2023;14:1077236.
9. Carsetti R, Zaffina S, Piano Mortari E, Terreri S, Corrente F, Capponi C, Palomba P, Mirabella M, Cascioli S, Palange P, et al. Different Innate and Adaptive Immune Responses to SARS-CoV-2 Infection of Asymptomatic, Mild, and Severe Cases. Front Immunol. 2020;11:610300.
10. Arunachalam PS, Wimmers F, Mok CKP, Perera R, Scott M, Hagan T, Sigal N, Feng Y, Bristow L, Tak-Yin Tsang O, et al. Systems biological assessment of immunity to mild versus severe COVID-19 infection in humans. Sci (New York NY. 2020;369(6508):1210–20.
11. Phetsouphanh C, Jacka B, Ballouz S, Jackson KJL, Wilson DB, Manandhar B, Klemm V, Tan HX, Wheatley A, Aggarwal A, et al. Improvement of immune dysregulation in individuals with long COVID at 24-months following SARS-CoV-2 infection. Nat Commun. 2024;15(1):3315.
12. Pandey M, Ozberk V, Eskandari S, Shalash AO, Joyce MA, Saffran HA, Day CJ, Lepletier A, Spillings BL, Mills JL, et al. Antibodies to neutralising epitopes synergistically block the interaction of the receptor-binding domain of SARS-CoV-2 to ACE 2. Clin Transl Immunol. 2021;10(3):e1260.
13. WHO. Clinical management of Covid-19. 2020.
14. Finck R, Simonds EF, Jager A, Krishnaswamy S, Sachs K, Fantl W, Pe'er D, Nolan GP, Bendall SC. Normalization of mass cytometry data with bead standards. Cytometry A. 2013;83(5):483–94.
15. Kotecha N, Krutzik PO, Irish JM. Web-based analysis and publication of flow cytometry experiments. *Curr Protoc Cytom* 2010, Chap. 10:Unit10 17.
16. Amir el AD, Davis KL, Tadmor MD, Simonds EF, Levine JH, Bendall SC, Shenfeld DK, Krishnaswamy S, Nolan GP. Pe'er D: viSNE enables visualization of high dimensional single-cell data and reveals phenotypic heterogeneity of leukemia. Nat Biotechnol. 2013;31(6):545–52.
17. Van Gassen S, Callebaut B, Van Helden MJ, Lambrecht BN, Demeester P, Dhaene T, Saeys Y. FlowSOM: Using self-organizing maps for visualization and interpretation of cytometry data. Cytometry A. 2015;87(7):636–45.

18. Bruggner RV, Bodenmiller B, Dill DL, Tibshirani RJ, Nolan GP. Automated identification of stratifying signatures in cellular subpopulations. Proc Natl Acad Sci U S A. 2014;111(26):E2770–2777.
19. Juno JA, Tan HX, Lee WS, Reynaldi A, Kelly HG, Wragg K, Esterbauer R, Kent HE, Batten CJ, Mordant FL, et al. Humoral and circulating follicular helper T cell responses in recovered patients with COVID-19. Nat Med. 2020;26(9):1428–34.
20. Rossi CM, Lenti MV, Merli S, Di Sabatino A. Role of IgM Memory B Cells and Spleen Function in COVID-19. Front Immunol. 2022;13:889876.
21. Newell KL, Clemmer DC, Cox JB, Kayode YI, Zoccoli-Rodriguez V, Taylor HE, Endy TP, Wilmore JR, Winslow GM. Switched and unswitched memory B cells detected during SARS-CoV-2 convalescence correlate with limited symptom duration. PLoS ONE. 2021;16(1):e0244855.
22. Hale M, Netland J, Chen Y, Thouvenel CD, Smith KN, Rich LM, Vanderwall ER, Miranda MC, Eggenberger J, Hao L et al. IgM antibodies derived from memory B cells are potent cross-variant neutralizers of SARS-CoV-2. J Exp Med 2022, 219(9).
23. Sallusto F, Geginat J, Lanzavecchia A. Central memory and effector memory T cell subsets: function, generation, and maintenance. Annu Rev Immunol. 2004;22:745–63.
24. Crotty S. T Follicular Helper Cell Biology: A Decade of Discovery and Diseases. Immunity. 2019;50(5):1132–48.
25. Onodera A, Kokubo K, Nakayama T. Epigenetic and Transcriptional Regulation in the Induction, Maintenance, Heterogeneity, and Recall-Response of Effector and Memory Th2 Cells. Front Immunol. 2018;9:2929.
26. Ruterbusch M, Pruner KB, Shehata L, Pepper M. In Vivo CD4(+) T Cell Differentiation and Function: Revisiting the Th1/Th2 Paradigm. Annu Rev Immunol. 2020;38:705–25.
27. Kunzli M, Masopust D. CD4(+) T cell memory. Nat Immunol. 2023;24(6):903–14.
28. Nguyen QP, Deng TZ, Witherden DA, Goldrath AW. Origins of CD4(+) circulating and tissue-resident memory T-cells. Immunology. 2019;157(1):3–12.
29. Masopust D, Soerens AG. Tissue-Resident T Cells and Other Resident Leukocytes. Annu Rev Immunol. 2019;37:521–46.
30. Ait-Belkacem I, Cartagena Garcia C, Millet-Wallisky E, Izquierdo N, Loosveld M, Arnoux I, Morange PE, Galland F, Lambert N, Malergue F, et al. SARS-CoV-2 spike protein induces a differential monocyte activation that may contribute to age bias in COVID-19 severity. Sci Rep. 2022;12(1):20824.
31. Tsukalov I, Sanchez-Cerrillo I, Rajas O, Avalos E, Iturricastillo G, Esparcia L, Buzon MJ, Genesca M, Scagnetti C, Popova O, et al. NFkappaB and NLRP3/NLRC4 inflammasomes regulate differentiation, activation and functional properties of monocytes in response to distinct SARS-CoV-2 proteins. Nat Commun. 2024;15(1):2100.
32. You M, Chen L, Zhang D, Zhao P, Chen Z, Qin EQ, Gao Y, Davis MM, Yang P. Single-cell epigenomic landscape of peripheral immune cells reveals establishment of trained immunity in individuals convalescing from COVID-19. Nat Cell Biol. 2021;23(6):620–30.

33. Netea MG, Ziogas A, Benn CS, Giamarellos-Bourboulis EJ, Joosten LAB, Arditi M, Chumakov K, van Crevel R, Gallo R, Aaby P, et al. The role of trained immunity in COVID-19: Lessons for the next pandemic. Cell Host Microbe. 2023;31(6):890–901.
34. Cheong JG, Ravishankar A, Sharma S, Parkhurst CN, Grassmann SA, Wingert CK, Laurent P, Ma S, Paddock L, Miranda IC, et al. Epigenetic memory of coronavirus infection in innate immune cells and their progenitors. Cell. 2023;186(18):3882–902. e3824.
35. Pandori WJ, Padgett LE, Alimadadi A, Gutierrez NA, Araujo DJ, Huh CJ, Olingy CE, Dinh HQ, Wu R, Vijayanand P, et al. Single-cell immune profiling reveals long-term changes in myeloid cells and identifies a novel subset of CD9(+) monocytes associated with COVID-19 hospitalization. J Leukoc Biol. 2022;112(5):1053–63.
36. Ryan FJ, Hope CM, Masavuli MG, Lynn MA, Mekonnen ZA, Yeow AEL, Garcia-Valtanen P, Al-Delfi Z, Gummow J, Ferguson C, et al. Long-term perturbation of the peripheral immune system months after SARS-CoV-2 infection. BMC Med. 2022;20(1):26.
37. Vanneste D, Peng W, Liu Z, Hamaidia M, La Rocca R, Abinet J, Balthazar A, Perin F, Hego A, Cataldo D, et al. MafB is a conserved transcriptional regulator of macrophage development and functional identity across tissues and species. Immunity. 2026;59(3):559–76. e512.

Figures

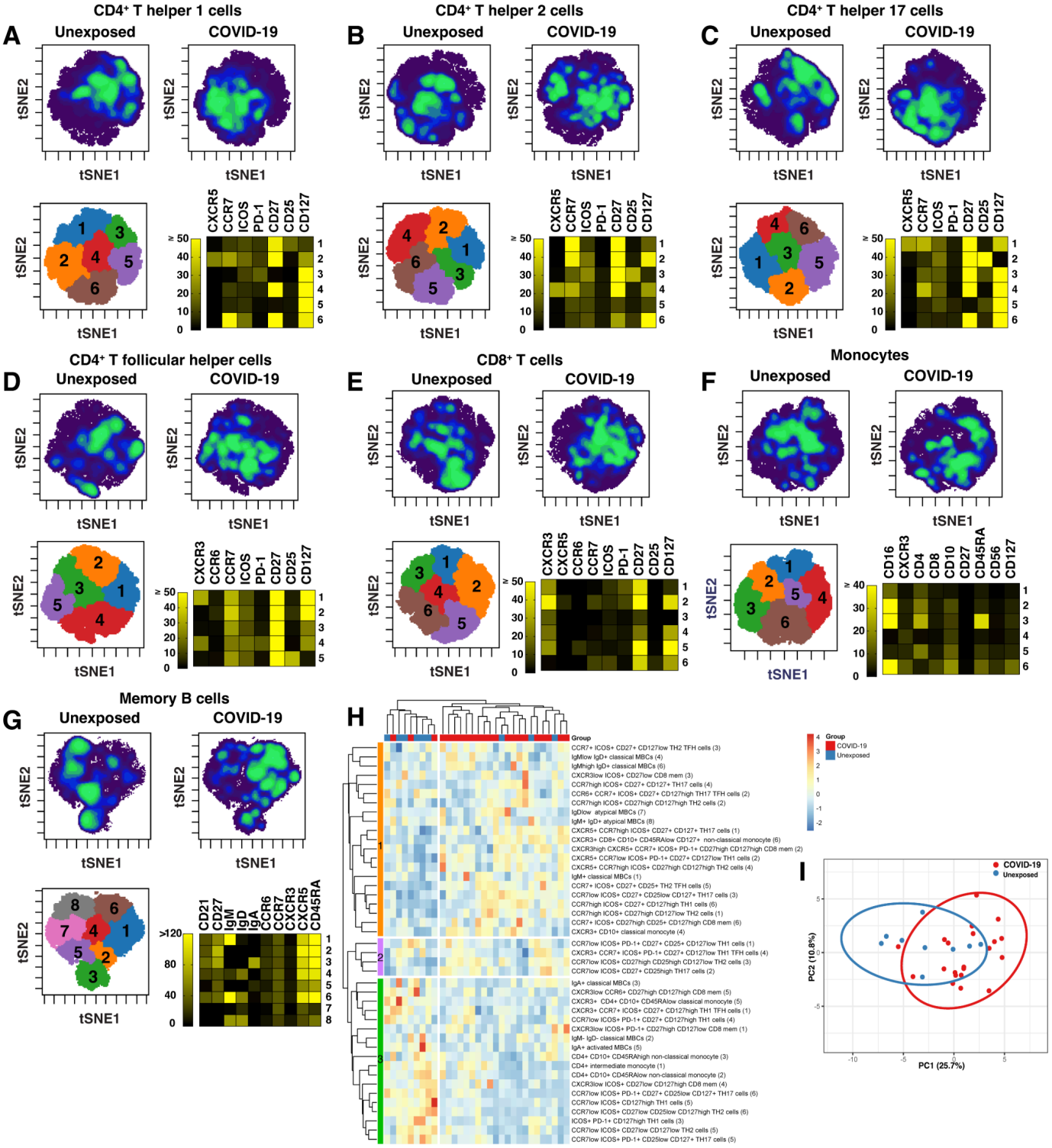


Figure 1

Identification of memory CD4$^+$ and CD8$^+$ T cells, MBCs and monocyte sub-populations in COVID-19 exposed individuals. **A-F**. PBMCs collected from convalescent COVID-19 cases (n=22) or unexposed controls (n=9) were stimulated with SARS-CoV-2 recombinant spike protein, stained with a panel of metal-labelled antibodies and analysed by CyTOF. tSNE analysis was performed and FlowSOM clustering was used to identify individual cell sub-populations within gated: **A**. T_{H1} memory CD4$^+$ T cells (CD19$^-$

$CD3^+CD4^+CD45RA^-CCR6^-CXCR3^+$), **B**. T_{H2}memory $CD4^+$ T cells ($CD19^-CD3^+CD4^+CD45RA^-CCR6^-CXCR3^-$), **C**. T_{H17} memory $CD4^+$ T cells ($CD19^-CD3^+CD4^+CD45RA^-CCR6^+CXCR3^-$), D. circulating memory T_{FH} cells ($CD19^-CD3^+CD4^+CD45RA^-CXCR5^+$), E. memory $CD8^+$ T cells ($CD19^-CD3^+CD8^+CD45RA^-$), **F**. monocytes ($CD3^-CD19^-CD14^+$). **G**. MBCs ($CD3^-CD19^+CD20^+CD10^-$) were identified among PBMCs without prior *in vitro* stimulation. The tSNE plots in the top panel display cell density and represent pooled data for each group, while the lower panel shows a projection of the FlowSOM clusters on a tSNE plot. Heatmaps show the median marker expression for each FlowSOM cluster. **H**. Unsupervised hierarchical clustering heatmap showing the frequency of all FlowSOM clusters across all clinical samples. **I**. Unsupervised multi-dimensional scaling of all populations identified by FlowSOM clustering across all clinical samples.

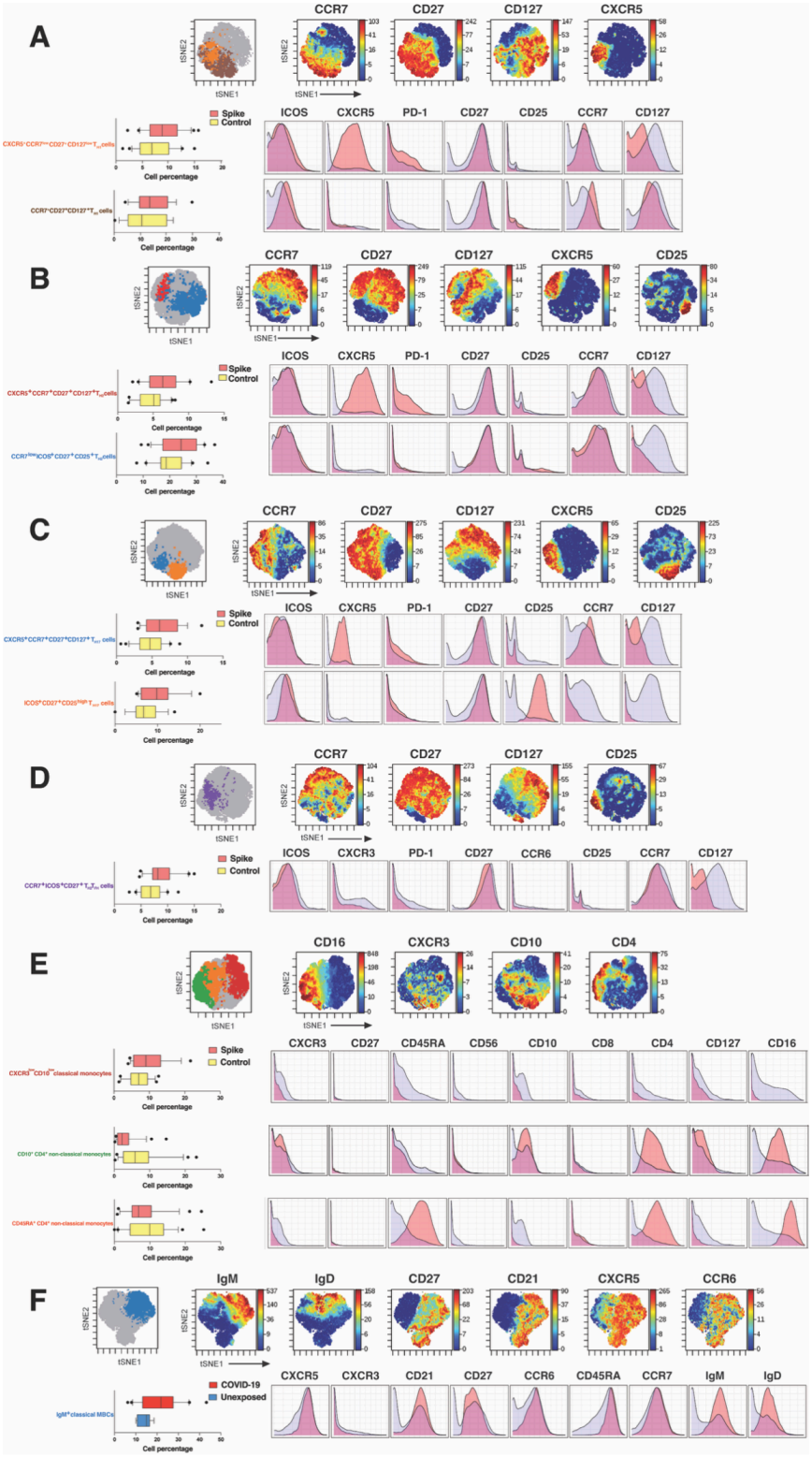


Figure 2

Subsets of T cells, monocytes and MBCs expanding in response to SARS-CoV-2 spike in COVID-19 convalescent individuals. **A-F**. Unsupervised identification of cell populations significantly expanding after *in vitro* restimulation with recombinant spike protein in COVID-19 convalescent individuals (n=22). Differentially abundant populations were identified among: (**A**) T_{H1} memory $CD4^+$ T cells; (**B**) T_{H2} memory

$CD4^+$ T cells; (**C**) T_{H17} memory $CD4^+$ T cells; (**D**) circulating memory T_{FH} cells and (**E**) monocytes. (**F**) MBCs were identified among PBMCs without prior *in vitro* stimulation. The top panels on the left show differentially abundant populations depicted in colours on a tSNE overlay, and the viSNE plots on the right-hand side from each top panel depict relevant marker expression on tSNE overlays. The lower left panels show the frequency of differentially abundant cell populations identified by CITRUS (FDR<5%). Boxes represent the 25^{th} to 75^{th} percentiles, show the range (minimum to maximum), and lines represent the median of 22 biological replicates. The lower right panels illustrate marker expression in differentially abundant populations (pink histograms), relative to background expression (lilac histograms).

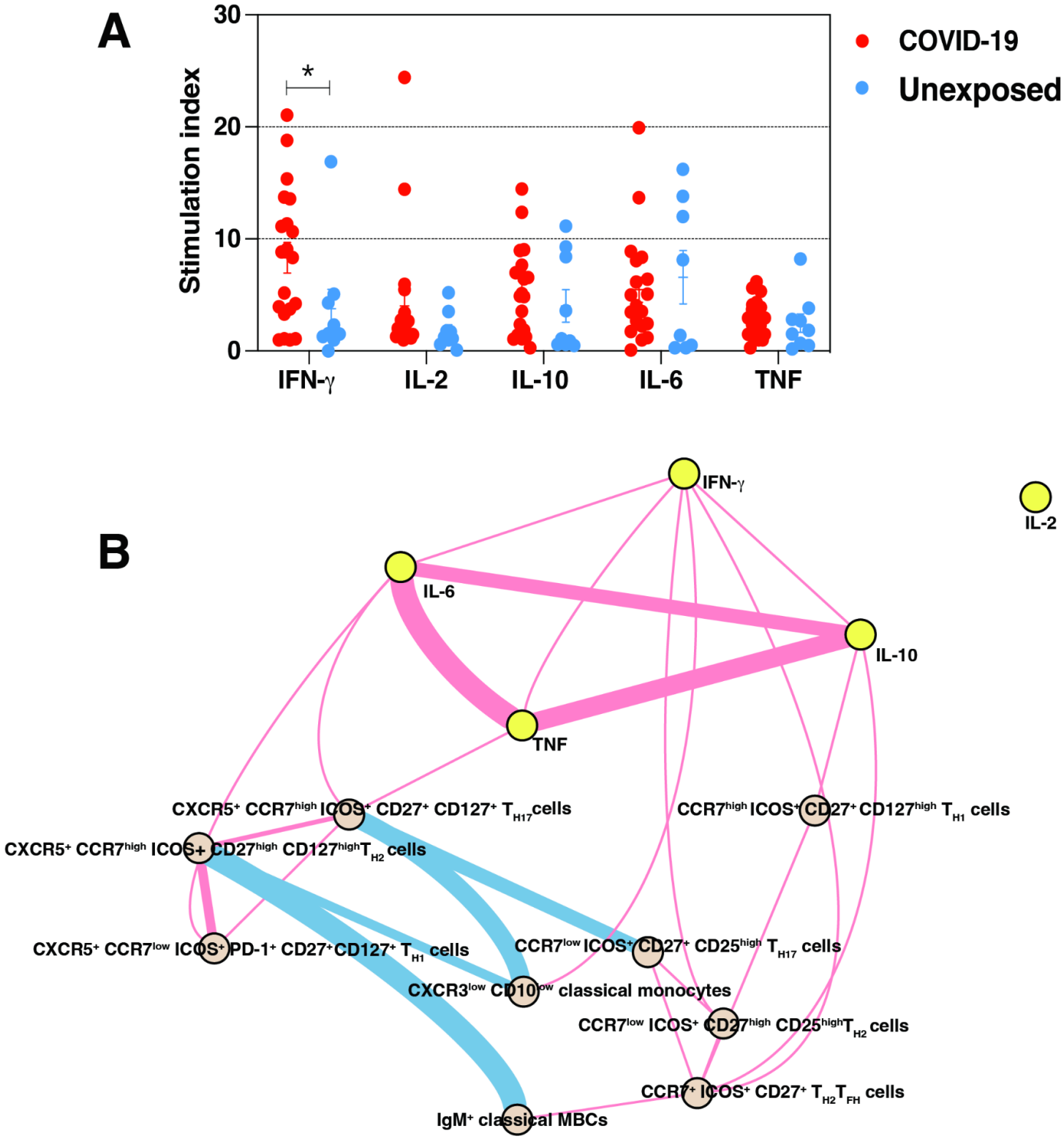


Figure 3

Correlation of cytokine responses with defined cell populations expanding in response to SARS-CoV-2 spike protein. **A**. PBMCs collected from convalescent COVID-19 cases (n=22) or unexposed controls (n=9) were stimulated with SARS-CoV-2 recombinant spike protein and cytokine responses were evaluated in cell culture supernatants, *p<0.05. **B**. Spearman rank correlation (Benjamini-Hochberg adjusted Spearman's Rho, FDR<5%) network between cell populations identified by CITRUS analysis and

cytokine responses visualised under force directed organic layout based on correlation strength. Pink lines represent positive correlations, and blue lines represent negative correlations. The distance between variables is determined by multidimensional scaling and the strength of the correlation is depicted by the width of lines connecting nodes in the network.

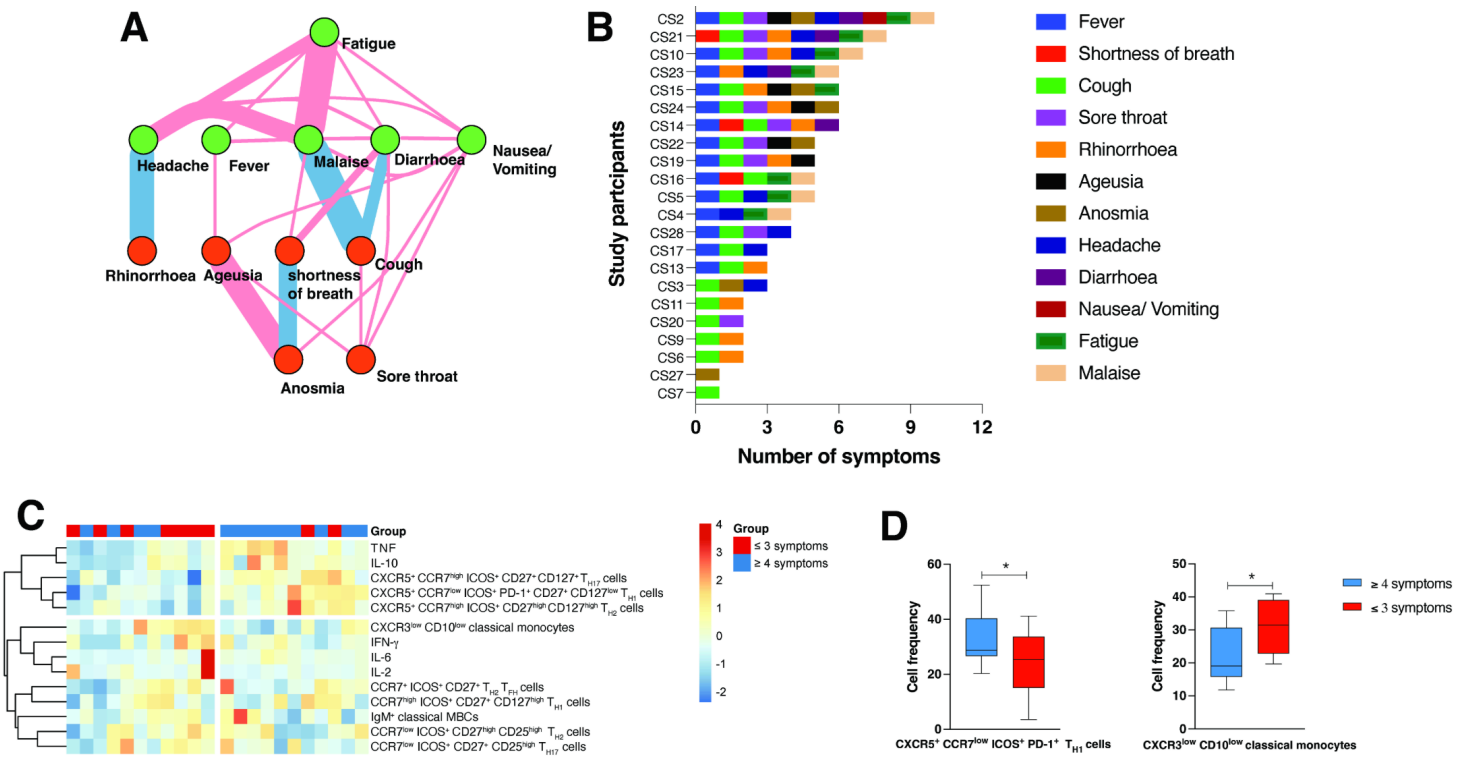


Figure 4

Associations between different COVID-19 presentations and cellular responses to SARS-CoV-2. **A**. Spearman rank correlation (Benjamini-Hochberg adjusted Spearman's Rho, FDR<5%) network between the incidence of COVID-19 symptoms experienced by naïve individuals (n=22) visualised under force directed organic layout based on correlation strength. Pink lines represent positive correlations, and blue lines represent negative correlations. The distance between categorical variables is determined by multidimensional scaling and the strength of the correlation is depicted by the width of lines connecting nodes in the network. **B**. Contingency graph showing individual incidence of COVID-19 symptoms across study participants. **C**. Unsupervised hierarchical clustering heatmap showing the frequency of cytokine responses and cell populations in PBMCs or study participants (n=22) significantly expanding in response to SARS-CoV-2 spike identified by CITRUS, across individuals experiencing ≤ 3 or ≥ 4 COVID-19 symptoms. **D**. Frequencies of $CXCR5^{+}CCR7^{low}ICOS^{+}PD\text{-}1^{+}$ T_{H1} cells and $CXCR3^{low}CD10^{low}$ classical monocytes in cases experiencing ≤ 3 or ≥ 4 COVID-19 symptoms, *p<0.05 Mann-Whitney test with correction for multiple comparisons.

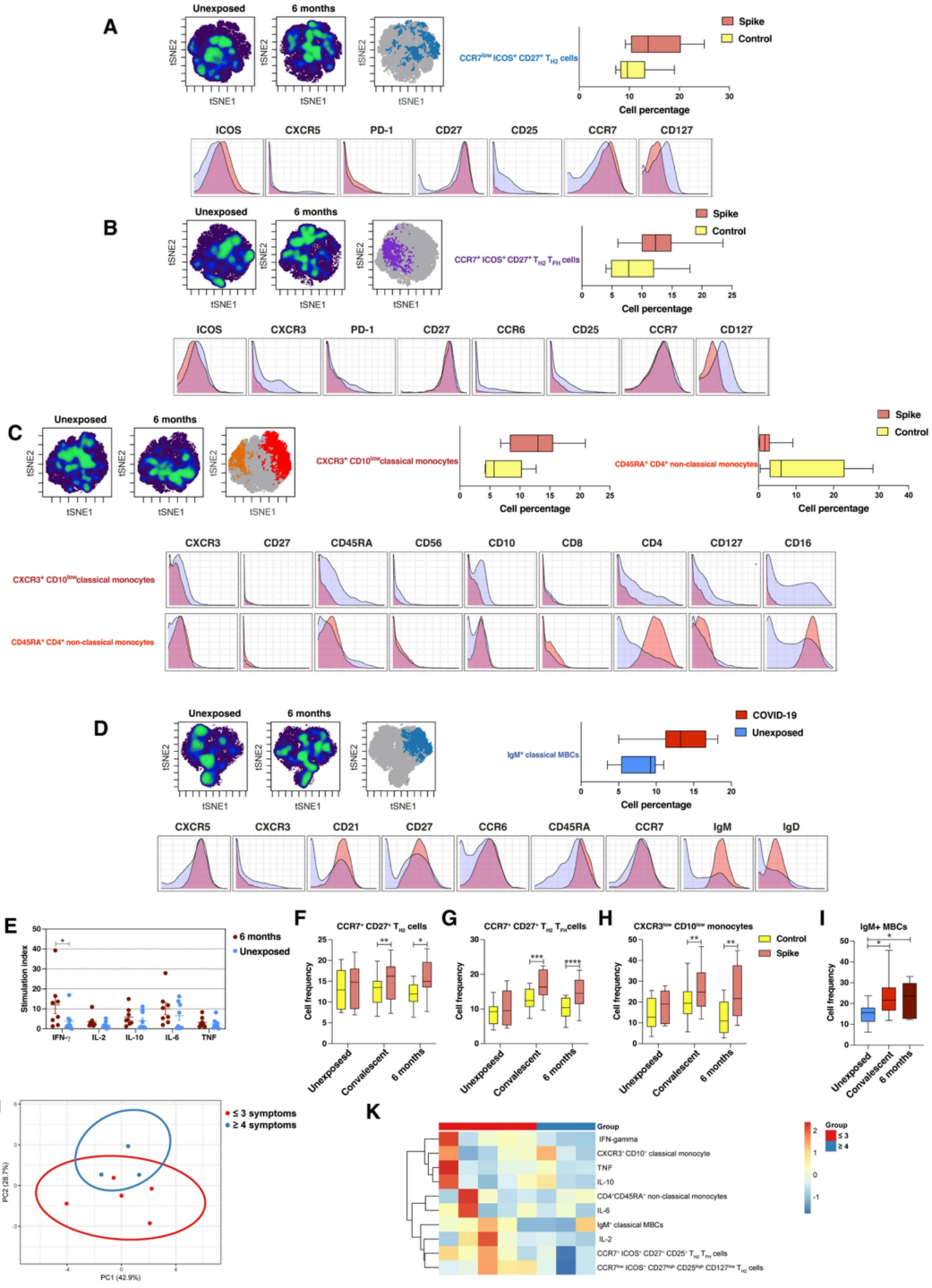


Figure 5

Mild COVID-19 presentation favour long-lived responses to SARS-CoV-2. A-D. PBMCs collected from 6 months after exposure to SARS-CoV-2 (n=8) or unexposed controls (n=9) were stimulated with SARS-CoV-2 recombinant spike protein, stained with a panel of metal-labelled antibodies and analysed by CyTOF. Unsupervised identification of cell populations significantly expanding after *in vitro* restimulation with recombinant spike protein in COVID-19 exposed individuals. Differentially abundant populations

were identified among: (**A**) T_{H2} memory $CD4^+$ T cells; (**B**) circulating memory T_{FH} cells and (**C**) monocytes. (**D**) MBCs were identified among PBMCs without prior *in vitro* stimulation. The top panels on the left show tSNE plots illustrating cell density and represent the pooled data. The middle panels show differentially abundant populations identified in colours on a tSNE overlay, and the graphs on the right-hand side from each top panel depict the frequency of differentially abundant cell populations identified by CITRUS (FDR<5%). Boxes represent the 25^{th} to 75^{th} percentiles, show the range (minimum to maximum), and lines represent the median of 8 (exposed) or 9 (unexposed) biological replicates. The lower right panels illustrate marker expression in differentially abundant populations (pink histograms), relative to background expression (lilac histograms). **E**. PBMCs from COVID-19 cases (n=8) or unexposed controls (n=9) were stimulated with SARS-CoV-2 spike protein and cytokine responses were evaluated in cell culture supernatants, *p<0.05. **F-H**. Frequencies of FlowSOM clusters defined in Fig. 1 corresponding to the phenotypes of $CCR7^+$ $ICOS^+$ $CD27^+$ (cluster 1 in Fig. 1B) T_{H2} cells (F), of $CCR7^+$ $CD27^+$ T_{H2}-polarised (cluster 5 in Fig. 1D) T_{FH} cells (G) or $CXCR3^{low}$ $CD10^{low}$ classical (cluster 4 in Fig. 1F) monocytes (H) were calculated before and after spike stimulation 3 weeks (n=22) and 6 months p.i. (n=8) with SARS-COV-2 and in unexposed controls (n=9). **I**. FlowSOM clusters of IgM^+ classical MBCs were identified among PBMCs (cluster 1 in Fig. 1G) without prior *in vitro* stimulation, *p<0.05, **p<0.01, ***p<0.005, ****p<0.001. Unsupervised multi-dimensional scaling (**J**) and hierarchical clustering heatmap (**K**) of cellular responses to SARS-COV-2 present at 6 months after exposure, across individuals experiencing ≤ 3 or ≥ 4 COVID-19 symptoms.

Supplementary Files

This is a list of supplementary files associated with this preprint. Click to download.

- AdditionalFiles.docx